Nuclear Physics A542 (1992) 559–578
North-Holland

NUCLEAR
PHYSICS A

Antideuteron annihilation on nuclei

J. Cugnon

Université de Liège, Institut de Physique au Sart Tilman, B.5, B-4000 Liège 1, Belgium

Received 14 November 1991
(Revised 8 January 1992)

Abstract: An investigation of antideuteron annihilation on nuclei within an intranuclear cascade (INC) model is presented. Two models are set up to describe the annihilation itself, which either implies the antideuteron as a whole and occurs at a single point, or which may be considered as two independent nucleon–antinucleon annihilations occurring at different points and different times. Particular attention is paid to the energy transferred from the pions issued from the annihilation to the nuclear system and to the possibility of having a multifragmentation of the target. The latter feature is investigated within a percolation model. The pion distribution and the energy distribution are also discussed. Predictions of proton multiplicity distributions are compared with experiment.

1. Introduction

Antiproton annihilation on nuclei has been much studied in the last years and has revealed many interesting facets. To cite the most important ones only, let us mention the interaction of a many-pion system with nuclei, strangeness production and the possibility of multifragmentation of nuclei by unconventional means [1]). Regarding this last aspect, it appears that antiproton beams provide a good way to study multifragmentation, complementary to proton and heavy-ion beams, presenting advantageous features, namely absence of compression and small linear and angular momentum transfers. At low energy, where scarce experiments have been performed, it turned out that the fragmentation of the target takes place in the subcritical regime. According to ref. [2]), the overcritical regime, where intermediate mass fragments are produced, would be reached when the incident $\bar{p}$ kinetic energy is larger than at least 1 GeV, or if antideuterons are used. The latter perspective is not simply academic, since the possibility of antideuteron beams at future accelerators is seriously envisaged [3]).

In this paper, we investigate the properties of antideuteron annihilation on nuclei, using the INC model, which has been proven to be very successful in describing antiproton annihilation on nuclei. In this first study, we focus our attention on the properties of target fragmentation induced by annihilation of antideuterons and in particular on the possibility that this fragmentation proceeds in the overcritical regime, in the sense of percolation theory (see below). As for our previous study

Correspondence to: Dr. J. Cugnon, Institut de Physique B.5, Sart Tilman, B-4000 Liège, Belgium.

of antiproton-induced multifragmentation [2]), we first examine the physical parameters which eventually determine the subsequent fragmentation, namely the energy transferred from the pions generated by the annihilation to the nucleus and the energy carried away by the ejected fast particles.

Our second purpose is to make predictions for the gross properties of the annihilation events, basically the particle multiplicities. We also want to investigate some features which are associated with the possibility of having a large energy release in a small region inside the nuclear volume. More precisely, we want to discuss the time evolution of the pion and energy densities.

2. The intranuclear cascade model for antideuteron interaction

Our INC model has been repeatedly described in the literature [2]). We need only discuss the features specific to the antideuteron case.

We built up two models for antideuteron interaction. In model A, a structureless antideuteron is supposed to annihilate *as a whole* on two nucleons, emitting pions uniformly in the invariant phase space. The distribution of the number of pions is assumed to follow the empirical law observed in the $\bar{p}p$ system, i.e. it depends upon the available energy only. It corresponds to a gaussian law with mean number $\langle n \rangle$ and variance σ [ref. [4])]:

$$\langle n \rangle = 2.65 + 3.65 \ln \sqrt{s} \,, \tag{2.1}$$

$$\sigma^2 / \langle n \rangle = 0.174 (\sqrt{s})^{0.40} \,, \tag{2.2}$$

where $\sqrt{s}$ is the c.m. energy expressed in GeV. The rescattering process initiated by the primordial pions is assumed to proceed as described in our previous works on antiproton annihilation on nuclei [5]).

In model B, the antideuterons are assumed to interact independently. Therefore, in some events, after a first antinucleon has been annihilated, the remaining antinucleon may scatter on the pions created in the first annihilation (and also, of course, on nucleons) before being annihilated on its turn, if it does not escape from the nucleus. The properties of the individual annihilations are supposed to be the same as the ones of the $\bar{N}N$ system. Initially, the antineutron and the antiproton are separated by a distance, which is chosen at random according to a distribution law given by the deuteron Hulthèn wave function [6]). The orientation of the relative vector is completely at random. The antideuteron so constructed is boosted with the appropriate velocity and impact parameter.

Both for models A and B, the reactions induced by nucleons and pions are described in our previous studies of $\bar{p}$-nucleus interaction [5,7]). However, the $\Delta N \rightleftarrows NN$ cross section and the Δ-lifetime have been slightly modified, as discussed in ref. [5]), to obtain a correct pion multiplicity at low energy. Above the Δ-resonance, the pions are allowed to interact elastically or inelastically with an average total

cross section of roughly 20–30 mb. The following reactions induced by antinucleons are introduced:

$$\bar{N}N \to \bar{N}N, \text{pions} \tag{2.3}$$

$$\bar{N}N \to \bar{N}\Delta, \bar{\Delta}N\,. \tag{2.4}$$

Cross sections for processes (2.3) are taken from experiment, whereas those for processes (2.4) are taken equal to the $NN \to N\Delta$ cross section. Finally, we also introduced

$$\pi\bar{N} \to \bar{\Delta}, \pi\bar{N}\,, \tag{2.5}$$

$$\bar{\Delta} \to \pi\bar{N}\,, \tag{2.6}$$

$$\bar{\Delta}N \to \bar{\Delta}N, \bar{N}N\,. \tag{2.7}$$

Cross sections for reactions (2.5) and (2.6) and the $\bar{\Delta}$ lifetime are taken the same as for their respective charge conjugate processes. The $\bar{\Delta}N$ reaction cross sections are taken the same as those for the ΔN system. This assumption is the most reasonable one, in view of the lack of experimental information.

We neglect strangeness production as well as mesonic resonances, assuming that both nucleon and pion inelastic collisions lead to pion production only. Furthermore, in order to keep the model as simple as possible, we do not treat explicitly the inelastic scattering (pion production) of the incoming antinucleons. In fact, the latter being very probably followed by annihilation, we assume that the antinucleons can be annihilated with an effective interaction

$$\sigma_a^{\text{eff}} = \sigma_a + \frac{\sigma_a}{\sigma_a + \sigma_p}\sigma_p\,, \tag{2.8}$$

where σ_a and σ_p are the experimental annihilation and (pion) production cross sections. Formula (2.8) represents a first chance plus second chance scenario. This procedure does not follow the correct energy evolution of a propagating antinucleon. The energy that would be lost for creating a pion is no longer available in the subsequent annihilation. However, it has been checked in ref. [8]) that the total number of pions produced, in an inelastic scattering followed by annihilation, is very nearly the same as the one of those produced by annihilation alone, at least for an energy up to 4 GeV.

To summarize our approach, we basically assume that the re-interaction of the annihilation products can be described, as for the antiproton case, by the INC model. In addition we mainly simplify the reaction scheme by assuming (1) no strangeness production, (2) inelasticity of incoming antinucleons describable by (2.8), and (3) pion and nucleon inelasticities proceeding through pion production only. We finally make two model assumptions for the antideuteron annihilation itself. Model A might be considered as a limit of model B when the two antinucleons are close to each other inside the deuteron. Notice, however, that the average number of primordial pions is not the same in the two cases, since the c.m. energy of the

$\bar{d}$–2N system is transformed into pions in a single step in model A, and in two steps in model B, and since relation (2.1) is not linear in the available annihilation energy. Model A is thus expected to produce less pions than model B in central collisions.

3. Energy transfer

3.1. INTRODUCTION

A key quantity in the study of the reaction of the nuclear system to the annihilation is the energy transferred from the pion system to the nuclear (baryonic) system. In all generality, one has at the end of the collision

$$W_{\rm inc} + W_{\rm T} = W_{\bar{\rm N}} + W_{\rm ej} + W_{\rm res} + W_{\pi}\,, \tag{3.1}$$

where $W_{\rm inc}$ is the antideuteron incident energy, $W_{\rm T}$ the target total energy, $W_{\bar{\rm N}}$ the energy of the possibly remaining antinucleon, $W_{\rm ej}$ the energy of the ejected nucleons, $W_{\rm res}$ the total energy of the target residue, and W_{π} the energy of the pion system. In an independent-particle model (like the INC model), relation (3.1) holds when the r.h.s. is taken at any time after the beginning of the collision process. It also holds event by event and for averages over events as well. It is more transparent if we rewrite it after taking account of baryon number conservation, which writes

$$A_{\rm T} - 2 = -\bar{\rm N} + A_{\rm ej} + A_{\rm res}\,, \tag{3.2}$$

where $\bar{\rm N}$ denotes the number of possibly remaining antinucleons, the meaning of the other symbols being obvious. Calling $E_{\rm i} = W_{\rm i} - A_{\rm i} m_{\rm N}$, for i = T, ej, res, the binding energy of the respective baryonic systems, we may combine eqs. (3.1) and (3.2) and write ($c = 1$)

$$W_{\rm inc} + 2M_{\rm N} = W_{\bar{\rm N}} + \bar{\rm N} M_{\rm N} + E_{\rm ej} + E^* + (E^0_{\rm res} - E^0_{\rm T}) + W_{\pi}\,, \tag{3.3}$$

where the index 0 refers to the ground state, and where the residual excitation energy E^* is given by

$$E_{\rm res} = E^* + E^0_{\rm res}\,. \tag{3.4}$$

Relation (3.3) shows that when the two antinucleons annihilate, the energy liberated, roughly the left-hand side of (3.3), is eventually distributed among the ejectiles, the pionic system and the excitation of the target remnant (if we disregard the difference between $E^0_{\rm res}$ and $E^0_{\rm T}$). In the INC model, the ground state energies are due to Fermi motion energy and the potential energy of the particles in a constant well of 40 MeV depth, which is a reasonable assumption for not too large depletion of the target.

In the INC model, the annihilation energy $W_{\rm ann}$, i.e. the energy converted into pions in the annihilations, is equal to the energy of the annihilating particles. In model A, $W_{\rm ann}$ slightly differs from the l.h.s. of the eq. (3.3) because of the Fermi motion of the two annihilating nucleons. In model B, it is given by

$$W_{\rm ann} = W^1_{\rm ann} + P_2 W^2_{\rm ann}\,, \tag{3.5}$$

where P_2 is the probability of having a second annihilation and where $W_{\rm ann}^{1,2}$ are the available energy in the respective annihilations. It may significantly be less than the l.h.s. of eq. (3.3) when only one of the antinucleons annihilates ($P_2 = 0$) or when the second antinucleon is substantially slowed down before annihilating.

In both model A and model B, the energy transfer $W_{\rm tr}$ is defined as

$$W_{\rm tr} = W_{\rm ann} - W_\pi . \tag{3.6}$$

It represents the energy lost by the pion system and thus, gained by the baryonic system.

3.2. TIME DEPENDENCE

In fig. 1 we show the time evolution of the various quantities entering eq. (3.3), $t = 0$ corresponding to the $\bar{\rm d}$ annihilation in model A and to the first antinucleon annihilation in model B. The pattern is rather the same for the two models. The pion system transfers energy to the baryonic system in roughly 10 fm/c, in the particular case of fig. 1. The excited nuclear system releases its energy by ejecting fast nucleons up to $t \approx 20$–25 fm/c, after which the system loses energy at a much slower rate, very much akin to evaporation. This situation is similar to what happens

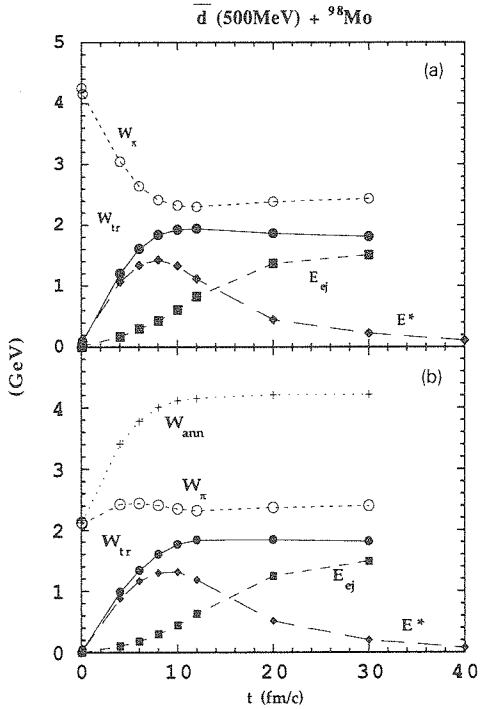

Fig. 1. Time evolution of the various quantities entering eq. (3.3) for central ($b = 0$) antideuteron annihilation on ^{98}Mo at 500 MeV. (a) model A, (b) model B.

in antiproton annihilation on nuclei. In model A, the whole process can clearly be divided into the following sequence: annihilation, transfer from the pion system to the nuclear system, ejection of fast particles, break-up and evaporation. In model B, there is a slight difference, coming from the non-simultaneity of the annihilations, which is reflected by the increase of the average annihilation energy at small times (in model A, the value of W_{ann} is equal to the pion energy at $t = 0$).

3.3. ENERGY DEPENDENCE

In fig. 2, we display the dependence upon the incident energy of the *final* values of the quantities entering eq. (3.3), for central collisions on a ^{98}Mo target. There is no very drastic difference between models A and B. One observes a continuous increase of the energy transfer and of the energy of the ejectiles, as more or less expected. However, the energy transfer is more efficient in model A at low and high incident energy. At low energy, this comes from the fact the remaining antinucleon (in model B) can be kicked out of the nucleus by the pions issued from the first annihilation. The survival probability is given in fig. 3. At high energy, the antinucleon

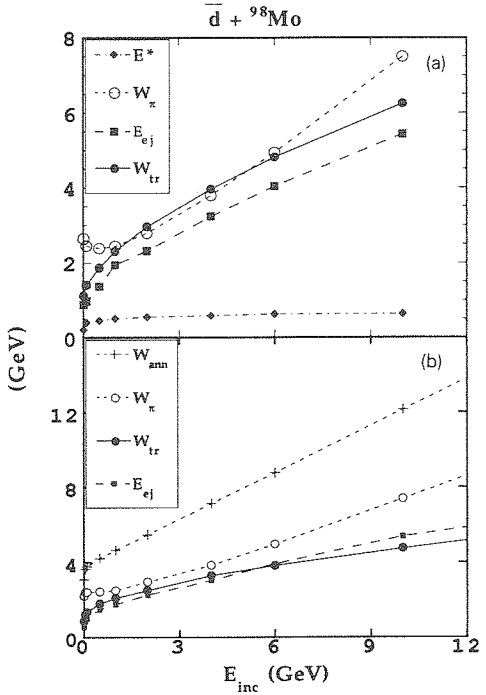

Fig. 2. Final values of the various quantities entering eq. (3.3) for central ($b = 0$) antideuteron annihilation on ^{98}Mo at various incident antideuteron kinetic energies E_{inc}. (a) Model A, (b) model B. For the sake of clarity, W_{ann} (roughly the l.h.s. of eq. (3.3) in model A) is not shown in the upper part and E^* (roughly the same as in model A) is not shown in the lower part.

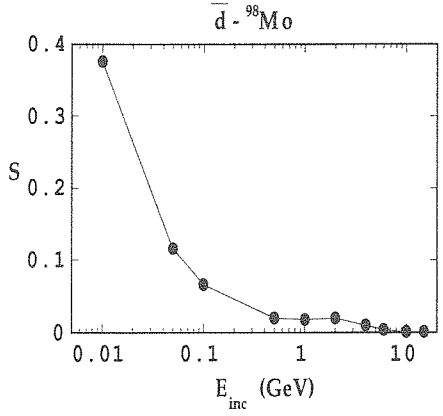

Fig. 3. Survival probability for the second antinucleon after the annihilation of its partner in the incoming antideuteron, in model B, as a function of the incident antideuteron kinetic energy. The figure refers to central ($b = 0$) antideuteron collisions with a ^{98}Mo target.

which survives for a while (in model B) loses energy before annihilating, giving rise to a smaller value of W_{ann} and therefore to a smaller value of W_{tr}. One may notice that in this case, E_{ej} may be larger than W_{tr}. This comes from the fact that then the nuclear system receives energy not only from the pions, but also from the surviving antinucleon itself.

It is also interesting to look at the efficiency coefficient for the energy transfer, i.e. at the ratio W_{tr}/W_{ann}. It is shown in fig. 4. It is worth to notice that this ratio never exceeds 0.55 even for central collisions. It first increases with energy and then slightly decreases above, say, 4 GeV. This behaviour results from an intricate interplay between geometry and the properties of the pions. At very low energy, some pions may escape from the nucleus because the annihilation is very peripheral. The interacting pions being roughly in the Δ-region, i.e. having the required kinematics to form Δ's with a huge cross section, they transfer much of their energy. When the incident energy increases, because of the Lorentz boost of the annihilation system, there are less and less non-interacting pions. But, progressively, the average energy of pions overtakes the Δ-region. They then interact with a much smaller cross section ($\approx$20 mb). Even more, their elastic scattering is rather forward peaked, which reduces the energy loss. This is, however, compensated by the inelastic scattering ($\pi N \rightarrow \pi\pi N$), which increases their number and degrades their average energy.

3.4. MASS AND IMPACT PARAMETER DEPENDENCE

The mass and impact parameter dependences are illustrated in figs. 5 and 6. The mass dependence is rather weak for large masses. The impact parameter dependence is rather expected. Note that for very peripheral collisions, we show average values for annihilation events only. One has to keep in mind that there is some probability

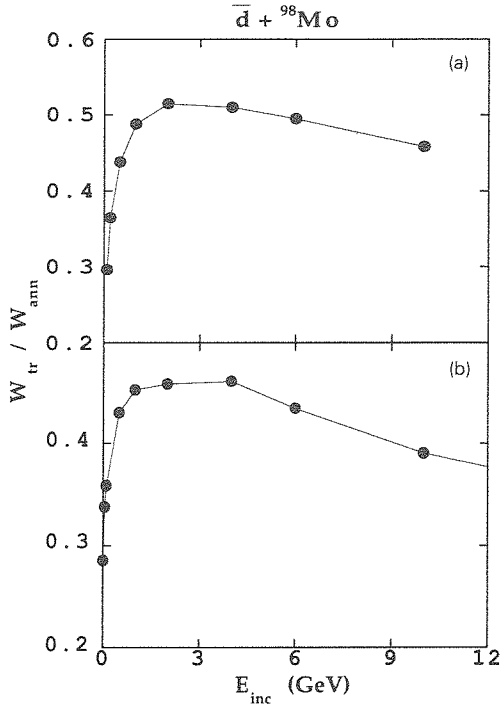

Fig. 4. Variation of the ratio between the energy transfer and the available energy in the annihilation, with the incident antideuteron kinetic energy for central ($b = 0$) antideuteron collisions with a ^{98}Mo target. (a) Model A, (b) model B.

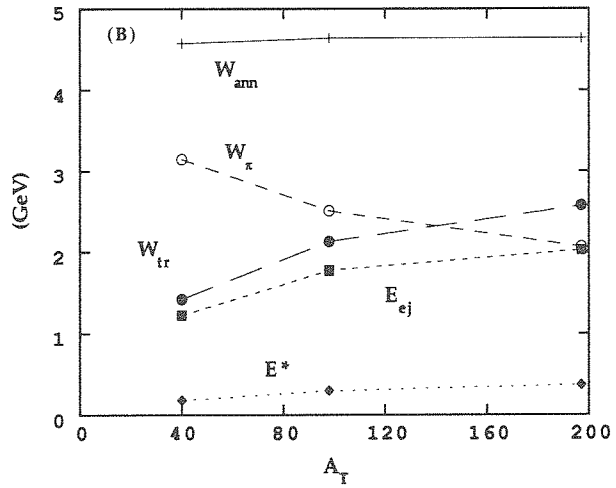

Fig. 5. Variation of the final values of the quantities entering eq. (3.3) with the target mass A_T, in model B. The figure refers to central ($b = 0$) antideuteron collisions of 1 GeV incident kinetic energy.

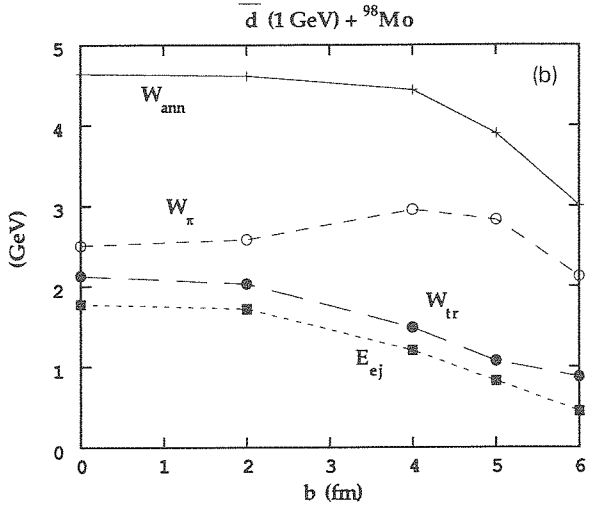

Fig. 6. Variation of the final values of the quantities entering eq. (3.3) with the impact parameter b, in model B. The figure refers to collisions of antideuterons of 1 GeV incident kinetic energy with a ^{98}Mo target.

for having no annihilation. Note the interesting variation of the final value of W_π. When b increases, there are less and less interacting pions: as a result, W_π increases. But, it eventually decreases because the available energy in the annihilation decreases, resulting from a larger and larger probability for one of the antinucleons to escape and avoid being annihilated.

4. Multifragmentation

4.1. PERCOLATION MODEL

We have seen in sect. 3.1 that (in the INC model), after the ejection of the fast particles, the nucleus releases energy at a much slower pace. One may think of this process as ordinary evaporation. However, at that time, the density distribution of the nucleus is quite uneven, since several nucleons have been ejected as a result of the pion propagation through matter: up to 30 nucleons in central collisions of 4 GeV antideuterons on Mo target. Therefore, the nucleus is expected to break up into pieces. This process cannot be handled directly by the INC model, since the latter neglects interaction energy, besides a constant average mean field. In order to have an idea of the properties of the multifragmentation process, we decided to use a percolation model [9]), which has been proven quite successful in other systems [10]). The latter assumes that the break-up of the nucleus is mainly determined by the geometric properties of the nucleon distribution at the end of the fast particle ejection (spallation) process. The method consists in constructing a minimum

spanning tree [11]) on the positions of the nucleons (event by event). Two nucleons are said to belong to the same cluster if the length of their link in the minimum spanning tree is smaller than a certain distance d. This procedure is rather heuristic, since the time at which the percolation procedure is applied is loosely defined, and since there is no a priori determination of the parameter d. In ref. [10]), it is shown that this method works rather well for proton-induced collisions in the 1-4 GeV range with $d = 2$ fm. Since we are interested here in pointing out the qualitative features of the multifragmentation only, we keep the same value for this parameter.

4.2. MASS YIELD

The mass yield obtained in our cascade plus percolation model is shown in fig. 7 for a typical case. One notices that there is practically no heavy residue in this particular case. In the percolation model language, one can say that the antideuteron annihilation leads to fragmentation in the overcritical regime. This is in contrast with the antiproton case, where the overcritical regime is reached in central collisions for incident energy larger than at least 1 GeV [ref. [2])]. With antideuterons, this regime has already set in at low energy.

The overcritical regime is possible at any antideuteron incident energy, although the excitation energy is not large (see figs. 1 and 2). It is not really larger than in the antiproton case (as far as this quantity can be precisely defined, as we already

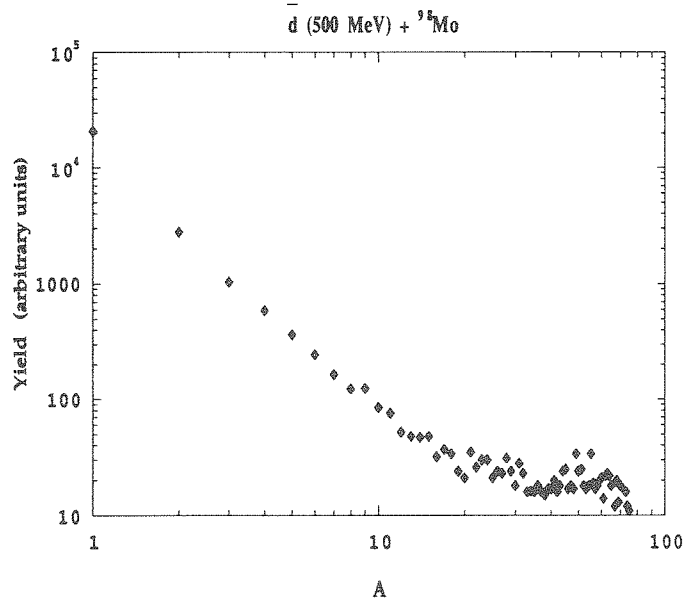

Fig. 7. Yield of fragments of mass number A emitted in central ($b = 0$) collisions of antideuterons of 500 MeV incident kinetic energy with a ^{98}Mo target (model B).

TABLE 1

Value of the parameter τ (E_{inc} in GeV)

$E_{inc}=0.01$	$E_{inc}=0.1$	$E_{inc}=0.5$	$E_{inc}=1$	$E_{inc}=2$	$E_{inc}=6$
1.90	2.17	2.03	2.03	1.94	1.91

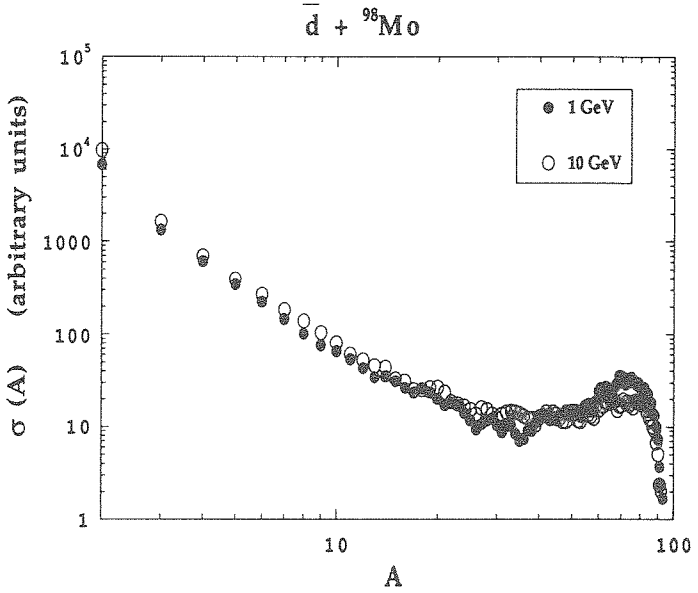

Fig. 8. Production cross section for a fragment of mass number A in antideuterons interactions with a ^{98}Mo target, in model B. The full dots correspond to an incident kinetic energy of 1 GeV, the open dots, to 10 GeV.

discussed in sect. 3). In fact, most of the extra transferred energy is carried out by the fast ejectiles. The reason comes from the fact that, in the antideuteron case, the pions have a larger average kinetic energy, compared to the antiproton case. It is generally believed that the excitation energy is the main parameter determining the

TABLE 2

Fraction of the annihilation cross section for various types of events (E_{inc} in GeV)

	$E_{inc}=1$	$E_{inc}=10$
No heavy residue	0.53	0.57
One IMF at least	0.22	0.26
Two IMFs at least	0.08	0.10

target fragmentation regime [11]). This is probably true in the heavy-ion case, where an (at least partially) equilibrated system is formed. On the contrary, in the antideuteron case, the nuclear distribution is not very uniform at the end of the fast ejection process. In a picturesque language, the pions produce several "holes" or "cracks" in the nucleus, which favours multifragmentation, at least if the percolation model provides a good picture of reality.

The small and intermediate A part of the mass yield, for say $A = 1$–25, follows very closely a power law $A^{-\tau}$. The exponent τ is given for central collisions in table 1. It does not change very much with energy.

The mass yield for antideuteron induced reactions, integrated over all impact parameters, is shown in fig. 8. In this case one can observe some heavy residues, corresponding, of course, to peripheral collisions. It is interesting to see how the events resulting from the annihilation are distributed with regard to the characteristics of the fragmentation (see table 2). About one half of the events correspond to multifragmentation, i.e. the absence of a "heavy" residue (here, defined as having a mass larger than two thirds of the original target). About one fourth of the events contains at least an intermediate mass fragment (IMF), here defined as having a mass number between 12 and 32. Finally, 10% of the events contain at least two IMF's.

In conclusion, the antideuteron annihilation leads to a fragmentation in the overcritical regime, rather independently of the energy, which can be characterized as being barely overcritical. Results of this section are given for model B only. Model A leads to a slightly more overcritical multifragmentation (e.g. slightly smaller values of τ).

5. Average multiplicities

In sect. 4, we have shown that most of the events can be characterized by the multifragmentation of the target, which results in the emission of slow fragments in the lab system. In order to provide a rough guide for possible future experiments, we pay here some attention to the multiplicities of fast particles. Table 3 gives the average multiplicity of pions and fast nucleons (here defined as having a kinetic energy over 60 MeV) for central collisions on a Mo target, both for model A and model B. The trends are roughly similar in both models. Model B yields more pions and model A yields more fast nucleons (at high energy at least), as expected.

An interesting result of table 3 is the turn-over in the evolution of the pion abundances: in both models A and B, pions are globally absorbed below 4 GeV, whereas there is a net increase at larger energy.

The present INC model does not distinguish between charges. However, if one assumes that the charge states of the final pions are in the same ratio N/Z as the nucleons (i.e. if one assumes charge equilibrium), one expects, in central collisions around 10 GeV, about 19 charged fast particles (on the average). We checked that for a $A = 197$ target, this feature raises to about 27.

TABLE 3

Pion and fast nucleon average multiplicities for central collisions on a Mo target

	E_{inc} (GeV)					
	0.1	1	2	4	6	10
Model A						
numbers of						
primordial pions	7.30	7.73	8.04	8.62	9.20	9.90
final pions	6.01	6.57	7.28	8.92	10.71	14.06
fast nucleons	8.04	11.08	13.92	17.32	20.08	23.28
Model B						
numbers of						
primordial pions	9.12	10.33	10.65	11.41	12.18	12.98
final pions	7.39	8.02	9.09	11.10	12.88	16.23
fast nucleons	6.00	11.48	14.00	16.16	16.72	18.80

6. Space-time distributions

6.1. PION DISTRIBUTION

One of the remarkable aspects of antideuteron annihilation is the creation of several pions in a small region of the nucleus. This observation is particularly relevant if the antideuteron annihilates as in model A. At very low energy, the pions are expected to recess from each other very quickly (in the lab system). At high energy, the pions remain close to each other for a while in the nucleus system, because of the Lorentz boost. The pion distribution, as calculated in our model A, is shown in fig. 9. The latter gives the distribution averaged over many events, but assuming a fixed annihilation point. This plot thus gives the probability distribution of finding a pion for the annihilation at the indicated point. Geometrically, the pion distribution looks like a wave developing from the annihilation site and propagating mainly in the forward direction.

One has to realize that fig. 9 depicts the probability distribution of the pions. In a given event, several pions will occupy positions at random in the shape of this distribution. Due to fluctuations, occasionally, a relatively large number of pions will travel in the nucleus very close to each other for a distance of a few fm. If this picture, dictated by energy–momentum conservation, Lorentz boost and the assumption of a point-like annihilation, is correct, one expects that these pions should behave coherently. This situation is qualitatively new, compared to what happens in the low energy regime. However, it is reasonable to believe that the behaviour of coherent pions in a small volume is basically describable in terms of resonances, like ρ and ω mesons. Therefore, it is not clear that this leads to new phenomena. If pions behave more like resonances, their energy loss may be substantially less than calculated here, since the cross section for resonances is about the same as

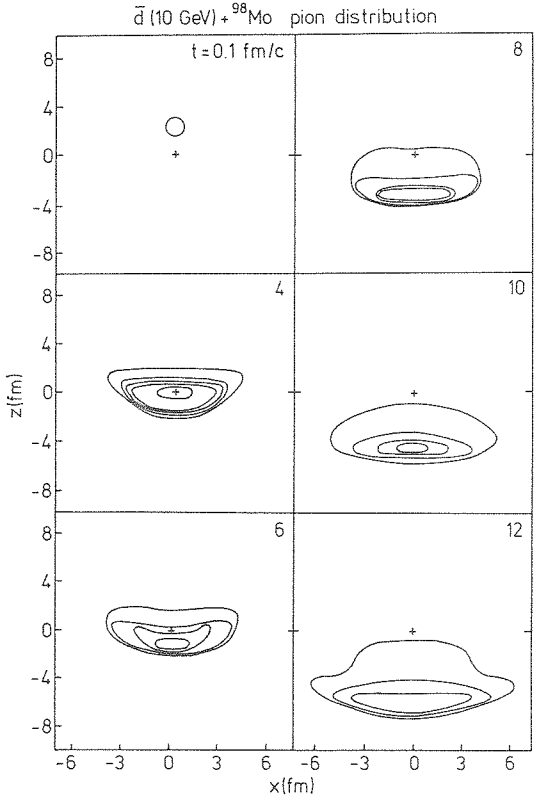

Fig. 9. Contour plot of the spatial pion distribution in the reaction plane for central ($b = 0$) collisions of 10 GeV incident kinetic energy antideuterons with a ^{98}Mo target, in model A. The various parts of the figure correspond to different times after the annihilation of the antideuteron. For each part, the successive contours display values of the density decreasing each time by a factor 2, starting from the innermost contours. The latter correspond to densities of 1.97, 0.49, 0.25, 0.125, 0.125 and 0.062 fm^{-3} for the six parts of the figure, respectively. The center of the target nucleus is indicated by the cross of the center of each part of the figure. The antideuteron is coming from above. See text for details.

those for pions in this energy range, which would mean that the equivalent "cross section per pion" will be smaller.

6.2. ENERGY DISTRIBUTION

An important point, already discussed in refs. [12,13]), is the energy density reached in the collision process. In the extreme view of a point-like annihilation, one would have an infinite energy density for an infinitely small time interval. However, it is physically meaningful to discuss energy density when considering a finite volume and not too small a time interval. For instance, if one looks for the possibility of having the necessary energy density for the formation of a quark-gluon plasma, it

is of no significance to realize this energy density in a volume whose linear dimension would be smaller than the correlation length in the plasma.

The energy density in a small volume Δv is given by

$$T_{00} = \frac{1}{\Delta v} \sum_{j \in \Delta v} p_0^{(j)}, \tag{6.1}$$

where $p_0^{(j)}$ is the fourth component of the four-momentum of particle j. It should be remarked that T_{00} contains the energy of motion of Δv as a whole (c.m. motion). The internal energy density has meaning in the comoving frame only. Roughly speaking [15]) it is given by T_{00}/γ^2, where γ is the Lorentz factor corresponding to the c.m. velocity of the comoving frame relative to the lab system: one factor γ comes from the transformation of the energy and the other from the transformation of the volume.

The distribution of T_{00} is given in fig. 10 for the same case as in fig. 9. The peak values of T_{00}/γ^2 are given by the heavy dots, at the various times indicated in the figure. One can see that the "critical" value of $2\,\mathrm{GeV}\cdot\mathrm{fm}^{-3}$ is reached in some region of the space-time. However, if one looks carefully, the linear dimension of this region (in the target frame) never exceeds 2 fm (even transversally, not shown in the figure). Furthermore, this region is not really thermalized. So, one can hardly believe that the antideuteron annihilation is a suitable means to create a quark–gluon plasma, in this energy range at least.

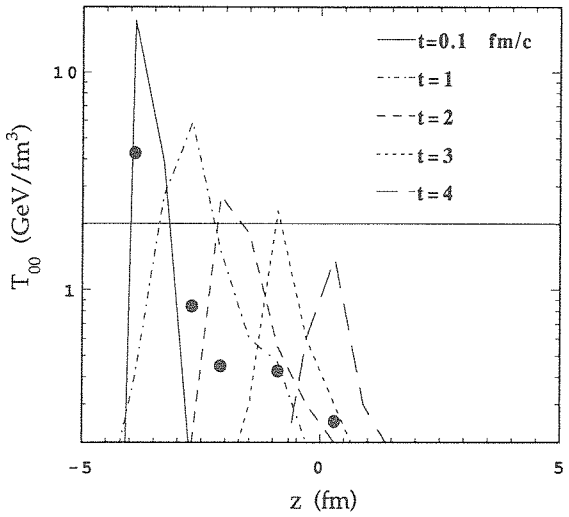

Fig. 10. Energy density profiles occurring at various times along the axis through the nucleus followed by the incident antideuteron in a central ($b=0$) collision at 10 GeV incident kinetic energy with a ^{98}Mo target. The centre of the nucleus is located at $z=0$ and the annihilation occurs at $t=0$. The antideuteron is coming from the left.

7. Antidelta annihilations

In our model B, antideltas can be produced either by interaction of the pions issued from the first annihilation and the surviving antinucleon, or by excitation of this antinucleon through a collision with one of the target nucleons. The antidelta can decay by emitting a pion and an antinucleon or they can annihilate on a target nucleon. On the average, at an incident energy of 1 GeV, an antidelta is produced in 29% of the events. It annihilates in 15% of the events and decays in another 14%. At 4 GeV incident energy, an antidelta is produced 24% of the time.

8. Comparison with experiment

There are rather scarce experimental data with antideuterons, and they have been obtained with poor quality beams. Antideuteron reaction cross sections have been measured for several nuclei in ref. [16]). Unfortunately, the latter measurements have been done at an incident energy of 11.6 GeV, where our model becomes rather uncertain. Nevertheless, we compare in fig. 11 our predictions for model B (at 10 GeV) with the data of ref. [16]). One can see that we underestimate the reaction cross section, and that we roughly reproduce the stripping cross section for the mechanism by which an antineutron is annihilated whereas the antiproton continues unperturbed. The absorption cross section seems to be larger than the value expected on purely geometrical considerations. On the other hand, the stripping cross section is roughly given by geometrical arguments.

We also compare with recent measurements on antideuteron annihilation on a ^{181}Ta target [17]) in figs. 12 and 13. In fig. 12, we display the calculated distribution

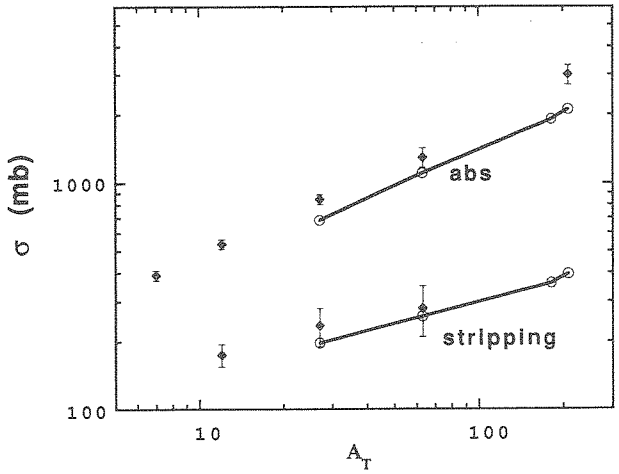

Fig. 11. Comparison of our predictions (model B) for the antideuteron absorption and stripping cross sections with the data of ref. [16]) for 13.3 GeV/c antideuterons. See text for details.

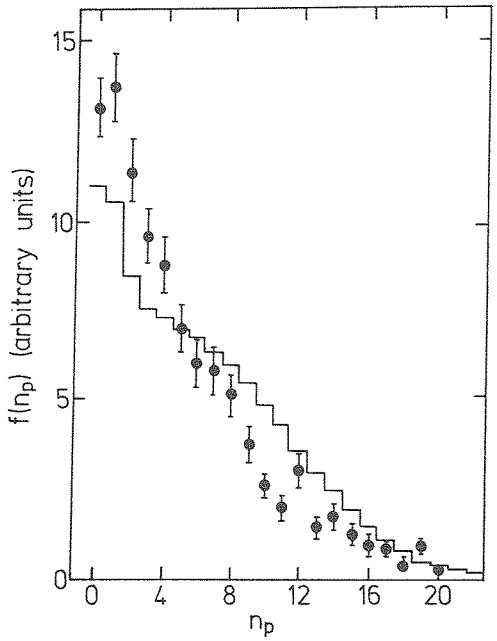

Fig. 12. Theoretical distribution of the proton multiplicity n_p (histogram) with the measurements of ref. [17]) for interaction of 12.2 GeV/c antideuterons with ^{181}Ta nuclei. See text for details.

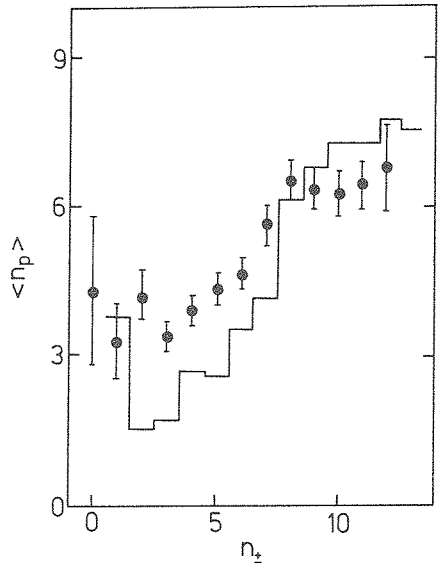

Fig. 13. Correlations between the number of charged pions $n_\pm$ and the average proton multiplicity in interaction of 12.2 GeV/c antideuterons with ^{181}Ta nuclei. Histogram: theoretical values, dots: data from ref. [17]).

of proton multiplicity, where we restrict to protons with a kinetic energy larger than 50 MeV, which corresponds more or less to the experimental cuts. Since our code does not distinguish between charged states, the protons are taken at random from the ejected nucleons with a probability equal to the Z/A ratio of the total system. One observes from fig. 12 that the agreement with experimental data is rather good, especially if one reminds that the experimental data are contaminated by π^--Ta events. That may explain the observed enhancement of small proton multiplicity events. In fig. 13, we display the calculated correlation between the $\pi^\pm$ multiplicity and the average proton multiplicity. Due to the limited quality of the experimental data, the agreement is rather good. One may notice, however, an experimental enhancement of the proton multiplicity for events with a small number of charged pions. This feature, already present in antinucleon data [18]) is not really reproduced by the INC calculations [see also ref. [17])]. It might indicate that for a small fraction of annihilation events (events with small $n^\pm$ are rather infrequent) the annihilation process has a tendency to transfer the available energy on a baryon-rich system, at least more than indicated by the INC model.

9. Discussion and conclusion

We have presented a first study, within the INC model, of the main features of antideuteron annihilation on nuclei. In order to introduce as less arbitrariness as possible regarding the unknown mechanism of the antideuteron annihilation, we have set up two models for antideuteron annihilation on nuclei. They differ on the properties of the annihilation itself: $\bar{\mathrm{d}}$-2N annihilation at a single point in model A, independent $\bar{\mathrm{N}}$N annihilations in model B. The reaction dynamics following and preceding the annihilation is rather simplified, although we introduced already a large number of reactions. We mainly disregarded three features in the energy range considered here: (1) strange particle production is neglected, (2) the possible inelastic scattering of incoming antinucleons (in model B) prior to annihilation is simply incorporated in an effective annihilation cross section, (3) mesonic resonances are ignored. As a result, the inelasticity of the whole collision process is ensured by the nucleon and pion scatterings. The inelastic scatterings are supposed to lead to pion and delta production only. This simplified dynamics is certainly grossly correct, up to, say $\approx$4 GeV incident energy, as discussed and explained in refs. [8,19]). Above this energy, our approach should be considered as an extrapolation only. However, the rather good agreement with the scarce existing data around 10 GeV/c indicates that the gross properties of the energy momentum flow are probably satisfactorily handled by our model, despite of its apparent crudeness.

We focused our attention to the energy transferred to the nuclear system after antideuteron annihilation and on the possible influence on the fragmentation of the target. We found that the energy transfer is in absolute value more than twice the one occurring in antiproton annihilation with the same incident kinetic energy [5]),

but, that the excitation energy left in the target residue after the fast ejectile emission process is roughly the same. This happens because primordial pions are more energetic and transfer their available energy to more energetic ejectiles (nucleons mainly). Nevertheless, because the number of primordial pions is always larger than in the antiproton case, the target residue has a larger chance to fragment. We have shown that, in central collisions at least, the multifragmentation of the target, i.e. the fragmentation without heavy residue, always occurs. Our results indicate, however, that the properties of the multifragmentation do not change very much with energy and that the fragmentation regime is barely overcritical: large mass yield exponent, relative importance of intermediate mass (and beyond) fragment yields, ... In conclusion, the antideuteron beams will allow the study of multifragmentation just in the overcritical regime. They do not seem to offer the possibility of exploring various patterns of multifragmentation easily.

We have found that, concerning these points (energy transfer and multifragmentation) models A and B yield roughly the same results, with the exception of a somehow larger pion yield for model B. The latter might be considered as more realistic since it also incorporates antideuteron stripping. However, it is conceivable that, due to quantum fluctuations, an antideuteron in some compact configuration may annihilate on two nearby nucleons, a process for which model A could be relevant. In the latter perspective, we also paid attention to the energetics of the reaction dynamics. We pointed out the possibility of having closely packed, possibly coherent pions travelling inside the nucleus. The properties of this particular system ought to be investigated further. We have shown that high energy density is reached in some region of space-time. This possibility was already underlined in ref. [13]). However, due to the limited dimensions of this excited system both in space and time, the antideuteron beams do not appear as a suitable means to study quark-gluon plasma, in spite of claims [14]) which have been made for the less favorable case of antiproton annihilation. Finally, we compared our results with the few experimental data. The agreement is rather encouraging.

References

1) C.B. Dover, in First Workshop on Intense hadron facilities and antiproton physics, ed. T. Bressani, F. Iazzi and G. Pauli (Editrice Compositori, Bologna, 1990) p. 55
2) J. Cugnon, Nucl. Phys. **B8** [PS] (1989) 255
3) A.I. Yavin, in First Workshop on Intense hadron facilities and antiproton physics, ed. T. Bressani, F. Iazzi and G. Pauli (Editrice Compositori, Bologna, 1990) p. 223
4) J. Cugnon and J. Vandermeulen, Ann. de Phys. **14** (1989) 49
5) J. Cugnon, P. Deneye and J. Vandermeulen, Nucl. Phys. **A500** (1989) 701
6) L. Hulthèn and M. Sugarawa, Handbuch der Physik **39** (1957) 1
7) J. Cugnon, P. Jasselette and J. Vandermeulen, Nucl. Phys. **A470** (1987) 558
8) J. Cugnon, P. Deneye and J. Vandermeulen, Phys. Rev. **C41** (1990) 1701
9) X. Campi, J. Phys. **A19** (1986) L917
10) J. Cugnon and C. Volant, Z. Phys. **A334** (1989) 435
11) J. Dorfan, Z. Phys. **C7** (1981) 349

12) C. Ngô, Nuclear matter and heavy ion collisions, Les Houches (1989), NATO ASI Series B, vol. 205, p. 231
13) W. Gibbs and D. Strottman, Proc. of Int. Conf. on antinucleon and nucleon-nucleon intersections, Telluride (1985)
14) J. Rafelski, Phys. Lett. **B207** (1988) 371
15) L.D. Landau and E.M. Lifshitz, Fluid mechanics (Pergamon, Oxford, 1975) p. 499
16) Yu.P. Gorin *et al.*, Sov. J. Nucl. Phys. **13** (1971) 192 [Yad. Fiz. **13** (1971) 344]
17) V.F. Andreyev *et al.*, Nuovo Cimento **103A** (1989) 1163
18) Ye.S. Golubeva, A.S. Iljinov, A.S. Botvina and N.M. Sobelevsky, Nucl. Phys. **A483** (1988) 539
19) J. Cugnon, P. Deneye and J. Vandermeulen, Phys. Rev. **C40** (1989) 1822